



## **Geographical expansion of Northeast Atlantic mackerel (*Scomber scombrus*) in the Nordic Seas from 2007 to 2016 was primarily driven by stock size and constrained by low temperatures**

**Olafsdottir, Anna H.; Utne, Kjell Rong; Jacobsen, Jan Arge; Jansen, Teunis; Óskarsson, Guðmundur J.; Nøttestad, Leif; Elvarsson, Bjarki Þ.; Broms, Cecilie; Slotte, Aril**

*Published in:*  
Deep-Sea Research. Part 2: Topical Studies in Oceanography

*Link to article, DOI:*  
[10.1016/j.dsr2.2018.05.023](https://doi.org/10.1016/j.dsr2.2018.05.023)

*Publication date:*  
2019

*Document Version*  
Peer reviewed version

[Link back to DTU Orbit](#)

*Citation (APA):*  
Olafsdottir, A. H., Utne, K. R., Jacobsen, J. A., Jansen, T., Óskarsson, G. J., Nøttestad, L., Elvarsson, B. Þ., Broms, C., & Slotte, A. (2019). Geographical expansion of Northeast Atlantic mackerel (*Scomber scombrus*) in the Nordic Seas from 2007 to 2016 was primarily driven by stock size and constrained by low temperatures. *Deep-Sea Research. Part 2: Topical Studies in Oceanography*, 159, 152-168.  
<https://doi.org/10.1016/j.dsr2.2018.05.023>

---

### **General rights**

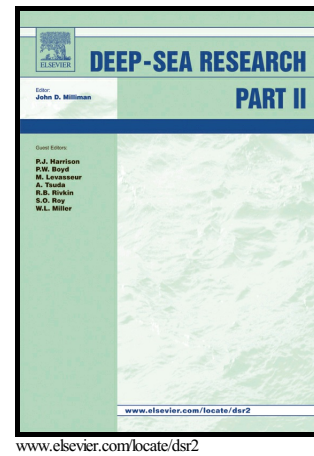
Copyright and moral rights for the publications made accessible in the public portal are retained by the authors and/or other copyright owners and it is a condition of accessing publications that users recognise and abide by the legal requirements associated with these rights.

- Users may download and print one copy of any publication from the public portal for the purpose of private study or research.
- You may not further distribute the material or use it for any profit-making activity or commercial gain
- You may freely distribute the URL identifying the publication in the public portal

If you believe that this document breaches copyright please contact us providing details, and we will remove access to the work immediately and investigate your claim.

Geographical expansion of Northeast Atlantic mackerel (*Scomber scombrus*) in the Nordic Seas from 2007 – 2016 was primarily driven by stock size and constrained by low temperatures

Anna H. Olafsdottir, Kjell Rong Utne, Jan Arge Jacobsen, Teunis Jansen, Guðmundur J. Óskarsson, Leif Nøttestad, Bjarki Þ. Elvarsson, Cecilie Broms, Aril Slotte



PII: S0967-0645(17)30259-X  
DOI: <https://doi.org/10.1016/j.dsr2.2018.05.023>  
Reference: DSR114454

To appear in: *Deep-Sea Research Part II*

Cite this article as: Anna H. Olafsdottir, Kjell Rong Utne, Jan Arge Jacobsen, Teunis Jansen, Guðmundur J. Óskarsson, Leif Nøttestad, Bjarki Þ. Elvarsson, Cecilie Broms and Aril Slotte, Geographical expansion of Northeast Atlantic mackerel (*Scomber scombrus*) in the Nordic Seas from 2007 – 2016 was primarily driven by stock size and constrained by low temperatures, *Deep-Sea Research Part II*, <https://doi.org/10.1016/j.dsr2.2018.05.023>

This is a PDF file of an unedited manuscript that has been accepted for publication. As a service to our customers we are providing this early version of the manuscript. The manuscript will undergo copyediting, typesetting, and review of the resulting galley proof before it is published in its final citable form. Please note that during the production process errors may be discovered which could affect the content, and all legal disclaimers that apply to the journal pertain.

Geographical expansion of Northeast Atlantic mackerel (*Scomber scombrus*) in the Nordic Seas from 2007 - 2016 was primarily driven by stock size and constrained by low temperatures.

Anna H. Olafsdottir<sup>a,c,d\*</sup>, Kjell Rong Utne<sup>b</sup>, Jan Arge Jacobsen<sup>c</sup>, Teunis Jansen<sup>d,e</sup>, Guðmundur J. Óskarsson<sup>a</sup>, Leif Nøttestad<sup>b</sup>, Bjarki Þ. Elvarsson<sup>a</sup>, Cecilie Broms<sup>b</sup>, and Aril Slotte<sup>b</sup>.

<sup>a</sup>Marine Research Institute, Reykjavik, Iceland;

<sup>b</sup>Institute of Marine Research, Bergen, Norway;

<sup>c</sup>Faroe Marine Research Institute, Torshavn, Faroe Islands;

<sup>d</sup>Greenland Institute of Natural Resources, Nuuk, Greenland.

<sup>e</sup>DTU AQUA – National Institute of Aquatic Resources, Kemitorvet, Building 202, 2800 Kgs. Lyngby, Denmark.

\*corresponding author: anna.olafsdottir@hafogvatn.is, tel: (+354) 575 2000, fax: (+354) 575

2001.

## Abstract

In the mid-2000s, summer feeding distribution of Northeast Atlantic mackerel (*Scomber scombrus*) in Nordic Seas began expanding into new areas. The present study explores how spawning stock biomass (SSB) and environmental conditions influenced this expansion using data from scientific surveys conducted in Nordic Seas from 1997 to 2016. During that period mackerel distribution range increased three-fold and the centre-of-gravity shifted westward by 1650 km and northward by 400 km. Distribution range peaked in 2014 and was positively correlated to SSB. Mackerel was present in temperatures ranging from 5°C to 15°C, but preferred areas with temperatures between 9°C and 13°C according to univariate quotient analysis. Generalized additive models (GAM) showed that both mackerel occurrence and density were positively related to location, ambient temperature, mesozooplankton density and SSB, explaining 47% and 32% of deviance, respectively. Mackerel relative mean weight-at-length was positively related to location, day-of-year, temperature and SSB, but not with mesozooplankton density, explaining 40% of the deviance. We conclude that geographical expansion of mackerel during the summer feeding season in Nordic Seas was driven by increasing mackerel stock size and constrained by availability of preferred temperature and abundance of mesozooplankton. Marine climate with multidecadal variability probably impacted the observed distributional changes but were not evaluated. Our results were limited to the direct effects of temperature, mesozooplankton abundance, and SSB on distribution range during the last two decades and should be viewed as such.

Keywords (min 4): Northeast Atlantic mackerel, *Scomber scombrus*, geographical expansion, Nordic Seas, spawning stock biomass, temperature, mesozooplankton abundance, mean relative weight-at-length.

## 1. Introduction

The Northeast Atlantic mackerel (*Scomber scombrus*) stock is a widely distributed, highly migratory, temperate schooling pelagic fish of great commercial importance (Trenkel et al., 2014). Mackerel become mature at age 2 to 3 years old, spawn annually, and most of the stock is less than 12 years old (ICES, 2016). Mature individuals undertake a seasonal migration along a south-to-north axis currently ranging from Gibraltar to Svalbard, approximately from latitude 36°N to 78°N (ICES, 2013; Nøttestad et al., 2016a). Their migration cycle is characterized by over-wintering, followed by spawning in the south from January to July, whereas they feed in the north during summer and fall (Belikov et al., 1998; Uriarte and Lucio, 2001; Iversen, 2002; Jansen et al., 2012, Utne et al., 2012; Nøttestad et al., 2016a). Prior to the mid-2000s, mature mackerel summer (June-August) distribution was restricted to the Norwegian Sea (east of longitude 10°W and south of latitude 72°N), the North Sea, and the shelf west of Scotland (Fig. 1).

From the mid-2000s through to the present, mackerel summer distribution expanded in two directions from the traditional feeding area in the central Norwegian Sea. During one decade, mackerel distribution edge expanded westward, along the south coast of Iceland and towards the east coast of Greenland by approximately 1500 km, and northward towards Svalbard by approximately 500 km (Berge et al., 2015; Jansen et al., 2016; Nøttestad et al., 2016a). This expansion was first noticed by the Icelandic commercial fishery for Norwegian spring-spawning herring (*Clupea harengus*) as its mackerel by-catch increased from 20 t in 2002 to 1700 t in 2006 (Astthorsson et al., 2012). By the summer of 2007, mackerel presence east and southeast of Iceland became more noticeable (Nøttestad et al., 2007) and a direct mackerel fishery began in

the eastern part of the Exclusive Economic Zone (EEZ) of Iceland (Astthorsson et al., 2012; Marine Research Institute, 2015). During the 20<sup>th</sup> century, there are a few reports of mackerel observations within the Icelandic EEZ from the commercial fleet and from historical records, however, the majority of observations were of a single individual fish (Lockwood, 1988; Astthorsson et al., 2012). This was a geographical distribution expansion but not a shift as mackerel density increased in the traditional feeding area in the Norwegian Sea and North Sea during the same period (Nøttestad et al., 2016a; van der Kooij et al., 2016).

Geographical distribution of migratory fish stocks is affected by abiotic and biotic environmental conditions, and population size as well as the individual's internal state mediated via motivations, constraints and feedbacks (Secor, 2015). Temperature is a major abiotic factor influencing geographical distribution of fish stocks in subarctic oceans (Drinkwater et al., 2014; Nye et al., 2014). Generally, in the northern hemisphere distribution shifts northward during warm periods and vice versa in cold periods (Sundby and Nakken, 2008; Nye et al., 2014). Furthermore, temperature can pose a direct constraint to a stock's distribution (Frank et al., 1996), as there is a physiological limitation to how cold/warm waters fish can tolerate (Brett, 1979). A major biotic factor is prey abundance and prey gradients, which have been positively linked to pelagic fish distribution during the feeding season (Broms et al., 2012).

It is well documented that fish stock size is frequently positively correlated to geographical distribution range (Lluch-Belda et al., 1989; Dragesund et al., 1997; Barange et al., 2009). Density-dependent habitat selection predicts that a population will expand into areas of lower habitat quality when stock size increase and retract into higher quality areas when stock size is small. MacCall's basin model postulates that increasing intraspecific competition in a core area reduces habitat quality to be equal to the quality of marginal areas, motivating individuals to move into previously unoccupied marginal areas (Fretwell and Lucas, 1969; MacCall, 1990). The

basin model thus predicts that density in the core area increases and that distribution range expands when stock size increases. Furthermore, that individual's somatic conditions are the same in the core area and in the marginal areas because habitat quality is the same (MacCall, 1990, Shephard and Litvak, 2004).

Marine climate influences geographical distribution of fish stocks and its effects operate on many time-scales that range from immediate (Frank et al., 1996) to multidecadal (Sundby and Nakken, 2008) and are often concomitant with changing population size (Drinkwater et al., 2003, 2006; Poloczanska et al., 2013). Climate change and multidecadal climate fluctuations like the subpolar gyre (Häkkinen and Rhines, 2004; Hatun et al., 2005), the Atlantic Multidecadal Oscillation (Schlesinger and Ramankutty, 1994), and the North Atlantic Oscillation (Hurrell, 1995) are linked to gradual changes in current circulation patterns and, in turn, nutrient concentrations (Hátún et al., 2017a) and sea temperature with cascading effects on productivity at all tropic levels (Drinkwater et al., 2003; Nye et al., 2014; Hátún et al., 2009, 2016, 2017b).

Temperature and prey availability are likely to influence mackerel distribution during the summer feeding season in the Nordic Seas. It is a temperate species, which relies on energy reserves collected during summer feeding as energy source for the over-wintering and spawning season (Lockwood, 1988; Olafsdottir et al., 2016). In the Nordic Seas, mackerel feed in the surface mixed layer, typically located in the upper 30 to 40 m and above the thermocline (Godø et al., 2004; Nøttestad et al., 2016b). It is an opportunistic predator with a wide range of prey species (Langøy et al., 2012; Bachiller et al., 2016). Main prey is calanoid copepods, and to a lesser extent euphausiids, amphipods, other planktonic crustaceans, pelagic molluscs and fish (Prokopchuk and Sentyabov, 2006; Langøy et al., 2012; Óskarsson et al., 2016; Bachiller, et al., 2016, 2018). Observations show that mackerel frequently occupy temperatures ranging from 8°C

to 14°C during the summer feeding period (Utne et al., 2012; Nøttestad et al., 2007, 2010 - 2015, 2016b, 2016c).

Recent work by Nøttestad et al. (2016a) suggested that the mackerel expansion in the Nordic Seas was positively related to stock size from 2007 to 2014, when stock size more than doubled. In the present paper, we expand this time series analysis to 1997 – 2016 and we also analyse the mechanisms behind the expansion. We assess how ambient temperature, prey abundance, and stock size influence mackerel summer distribution during range expansion from 2007 to 2016. Then we evaluate whether interannual temperature changes coincided with the sudden expansion in mackerel distribution by comparing temperature in the expansion areas before (1997-2006) and during (2007-2016) the expansion. Finally, we examine if habitat quality differs between the traditional feeding grounds in the Norwegian Sea and the recently invaded expansion areas. Somatic condition of individual mackerel, measured as relative mean weight-at-length, is used as proxy for habitat quality.

## **2. Material and methods**

### **2.1. Study area**

Oceanographic conditions in the Northeast Atlantic are influenced by topography and geostrophic currents coming from the south (temperate Atlantic waters) and from the north (cold Polar waters) and (Fig. 1). Atlantic water flows northwards into the Norwegian Sea, along the continental shelf edge towards Svalbard, and into the shelf area south and west of Iceland



(Blindheim and Østerhus, 2005). Polar water flows southward along the east coast of Greenland with branches diverted into cyclonic gyres in the Greenland Sea and the Iceland Sea (Blindheim and Østerhus, 2005). This causes a strong gradient of decreasing temperature from east-to-west at latitudes north of 65°N. The Norwegian Sea is dominated by warm Atlantic water, whereas the Greenland Sea and the Iceland Sea are dominated by cold Polar Water. The Northeast Atlantic has a strong seasonal cycle in biological productivity that is high in spring and summer but low in fall and winter (Gislason and Astthorsson, 1995; Melle et al., 2004). The major mesozooplankton groups are copepods, amphipods, euphausiids, other crustaceans, arrow worms, fish larvae, jellyfish and pelagic molluscs, but copepods are the most abundant group by far (Gislason, 2003, 2008; Gislason and Astthorsson, 2004; Melle et al., 2004).

## 2.2. *Biological data*

Standardized trawl hauls providing information on mackerel distribution and abundance were available from the International Ecosystem Summer Survey in Nordic Seas (IESSNS) from 2007 to 2016, excluding 2008 and 2009 (Table S1, Fig. 2a-h). No survey was conducted in 2008. In 2009, the survey focused on salmon research but not on mackerel (Nøttestad et al., 2009). The data were extracted from the Planning Group on Northeast Atlantic Pelagic Ecosystem Surveys (PGNAPES) database hosted at the Faroes Marine Research Institute, Torshavn, Faroe Islands. The survey was limited to a six-week period in July and early August, used a grid of mostly east-to-west transects or diagonal transects across the shelf edge, and distance between transects varied from 40 nmi to 60 nmi with trawl stations positioned every 30 nmi to 80 nmi along transects (for details see Nøttestad et al., 2016a). To provide comprehensive coverage of a

continually expanding mackerel distribution, survey coverage expanded westward and northward over the years (Nøttestad et al., 2016a).

At each station, a surface trawl was towed for approximately 30 minutes at a speed ranging from 4 to 5 kn. Floats were attached to the headline and the wings and kites on the top panel to secure its position at the surface and vertical trawl opening was usually with the range of 25 m to 35 m. The trawl catch was identified to species and weighted. Mackerel was caught at 1540 of 1868 stations sampled in 2007 and from 2010 to 2016 (Table S2). Thirty-eight of the 1540 stations with mackerel present did not have biological data. Mackerel density per station ( $DS$ ;  $\text{kg km}^{-2}$ ) was calculated as:

$$DS_i = \frac{C_i}{(TD_i * H_i)}, \quad (1)$$

where  $C$  is the mackerel catch (kg),  $TD$  is the distance of the trawl haul (km), and  $H$  is the horizontal opening of trawl (km) at station  $i$ .  $TD$  was calculated by multiplying tow time (h) by tow speed ( $\text{km h}^{-1}$ ). For the trawled area ( $\text{km}^2$ ), it was assumed that all mackerel were caught in the vertical dimension (see discussion about catchability in Nøttestad et al., 2016a).

Processing of trawl catches was as follows: total catch weighted, species composition determined by sorting the whole catch or by taking a subsample from the whole catch. Next, individual's total weight ( $\pm 0.5$  g) and total length (from the tip of the snout to the upper lobe of the pinched caudal fin;  $\pm 0.5$  cm; Hansen et al., 2018) were measured usually for a sub-sample of 50 – 100 mackerel. Number of individuals sampled per stations ranged from 1 to 524. In 2007 and from 2010 to 2016, 107,795 individuals were measured. Mackerel ranged from 18 cm to 47 cm in length. Shorter specimens ( $< 27$  cm) were eliminated from analysis as the  $\log_{10}$ weight-

$\log_{10}$ length relationship was heteroscedastic for that length range, i.e. majority of measurements were below the regression line. Elimination of shorter specimen does not influence our analysis as their proportion of the total number is small (3.8% of total number). For specimens  $> 27$  cm, deviation of each from the  $\log_{10}$ weight- $\log_{10}$ length linear relationship was calculated (Fig. 3) and this variable is defined as relative mean weight-at-length (Jakob et al., 1996).

Mackerel spawning stock biomass (SSB) was used as proxy for stock size during the summer feeding season in the Nordic Seas. The SSB estimate from the analytical assessment in 2016 was applied, which represents SSB at spawning time in May (ICES, 2016). The estimate of the mature part of the stock was used because the juveniles migrate to a lesser degree from the nursery areas into the study area (Jansen et al., 2015; Jansen and Burns, 2015; Nøttestad et al., 2016a).

### 2.3. *Mackerel geographical distribution*

To facilitate visualization of mackerel geographical expansion over time, the summer feeding range was split into three areas, the traditional feeding grounds in the Norwegian Sea, the westward expansion area (longitude west of  $10^{\circ}\text{W}$ ) and northward expansion area, located northward of the traditional feeding grounds (Fig. 1). Boundaries of the three areas were delineated from all available relevant resources (Fig. 1). For each year, the area occupied by mackerel and the centre-of-gravity (COG) of the distribution were calculated separately for the traditional feeding area and the westward expansion area. This was done to measure both directions of expansion, northward within the Norwegian Sea and westward outside the Norwegian Sea. In the Norwegian Sea, survey coverage was limited to latitudes north of  $62^{\circ}\text{N}$  in

some years (Nøttestad et al., 2016a). Therefore, calculations of area occupied and COG for the Norwegian Sea were limited to stations collected north of 62°N. In 2011, neither COG nor area occupied was calculated for the Norwegian Sea, only in the westward expansion area, as survey coverage was limited to latitudes south of 68°N.

To calculate area occupied, the area surveyed by the IESSNS was split into rectangles and the area occupied was the sum of all rectangles with mackerel present. Different rectangle size was used for the Norwegian Sea (2°latitude \* 4°longitude) and the westward expansion area (1°latitude \* 2°longitude) as distance between stations in the Norwegian Sea was occasionally too long (>60 nmi) for the smaller grid. Rectangle size (km<sup>2</sup>) was obtained using the “geo” package (version 1.4-3; Bjornsson et al., 2015) in R (R Core Team, 2014) and land areas were subtracted from rectangle size.

COG was calculated in four steps. The approach assumes that the earth is a perfect sphere where each position can be expressed by a 3-dimensional coordinate system (x,y,z). This approach handled decreasing distance between longitudes with increasing latitude without introducing bias in the calculations. The first step was to transform the data from CPUE per trawl haul to kg km<sup>-2</sup> (w) for each rectangle. A detailed description of the calculations is given in Nøttestad et al. (2016a). The next step was to convert latitude and longitude for each rectangle to Cartesian coordinates (cc). Then the mean weighted COG in Cartesian coordinates was calculated by the following equation:

$$cc_{x,y,z} = \frac{\sum_{i=1}^n cc_{i(x,y,z)} w_i}{\sum w_i}, \quad (2)$$

where  $i$  is the rectangle number. Finally, the COG given in Cartesian coordinates was transformed back to latitude and longitude.

Information on mackerel summer distribution in Nordic Seas from 1997 to 2007 were provided by the Institute of Marine Research, Bergen, Norway. This included all available CPUE surface trawl data from pelagic research trawl surveys executed in July in Nordic Seas during this period, in total 672 stations. Data were available for five of the ten years: 1997, 1998, 2002, 2003, and 2006. For these five years, gear type varied between years, but was the same for all vessels within each year. Hence, gear catchability does not affect calculated COG as the same trawl type was used by all vessels within each year. Area occupied and COG were calculated for those years using the same method as for the later period. For details of data collection methods see Utne et al. (2012). No mackerel were assumed to have existed in the westward expansion area prior to 2007 as only small number of individuals were recorded there from 1997 to 2006 in the commercial fishery targeting herring (Astthorsson et al., 2012).

#### **2.4. Environmental data**

At each IESSNS trawl station, temperature was measured with a CTD (Sea-Bird Electronics or SAIV A/S) from surface to 500 m depth, but the PGNAPES database only stores the data at 10 m depth intervals. The 10-m depth was considered representative for the part of the water column sampled by the trawl (surface to 25-35 m depth). The CTD was not employed at 92 of the total 1868 trawl stations. Mesozooplankton were sampled with vertical hauls using a WP-2 net (56 cm in diameter) from 200 m depth to the surface at each station. The mesh size of the net was 180  $\mu\text{m}$  or 200  $\mu\text{m}$  following IESSNS standards and sampling speed was  $0.5 \text{ ms}^{-1}$  (ICES,

2015). The mesozooplankton samples were split into two parts, one was frozen for weighing dry weight on land. On land, the samples were dried for 24-hours at 70°C and dry weight measured to the nearest mg (ICES, 2015). Mesozooplankton samples were collected at 1568 of the total 1868 trawl stations.

To measure annual temperature changes on the feeding grounds from 1997 to 2016, hypothetical expansion areas were visually defined from maps of mackerel presence from IESSNS 2010 to 2016 survey data (see Fig. 1). As a proxy for mixed-layer temperature, we used sea surface temperature (SST) derived from monthly optimum interpolation data, based on advanced, very high-resolution radiometer satellite data, version 2 (product: NOAA\_OI\_SST\_V2). These data have a spatial resolution of 1° latitude/longitude, temporal resolution of a month and were provided by the NOAA/OAR/ESRL PSD, Boulder, CO, USA, from their website at <http://www.esrl.noaa.gov/psd/data/gridded/data.noaa.oisst.v2.html> (downloaded in March 3, 2017). For detailed description of methods used to calculate SST see Reynolds and Smith (1995) and Reynolds et al. (2002). SST data were linked to mackerel summer feeding area by assigning monthly SST, from May to July, to every 1°latitude/longitude bin located within the defined area, in each year. To capture temperature changes from the beginning of the feeding migration until the peak of feeding, temperature values from May to July were included. The annual average monthly SST was calculated for each expansion area as the average of all SST values of geographical bins located in the area in that month and in that year.

## 2.5. Statistical analysis

A univariate quotient analysis was used to explore if mackerel frequency of occurrence and mackerel density, when present, was associated with a specific environmental condition (Lluch-Belda et al., 1991). Quotient analysis is used to detect environmental constraints on mackerel distribution. For a quotient analysis, continuous variables needed to be assigned categories. Observed temperatures ranged from  $-0.9^{\circ}\text{C}$  to  $14.8^{\circ}\text{C}$  at 10 m depth, and the temperature range was split into sixteen  $1^{\circ}\text{C}$  categories. Mesozooplankton dry weight ranged from  $1 \times 10^{-3} \text{ g m}^{-2}$  to  $43 \text{ g m}^{-2}$ , and was split into 22 categories, each being  $2 \text{ g m}^{-2}$ . However, distribution of mesozooplankton values into categories was not continuous for the whole data range as observations were missing in some categories above  $30 \text{ g m}^{-2}$ , hence quotient analysis was limited to dry weight  $<30 \text{ g m}^{-2}$  (eliminated 5 mesozooplankton stations of 1568). The quotient for mackerel presence ( $QP_i$ ) was calculated as:

$$QP_i = \frac{\left(\frac{p_i}{p}\right)}{\left(\frac{n_i}{n}\right)}, \quad (3)$$

where  $p_i$  is the number of stations with mackerel presence in category  $i$ ,  $p$  is the total number of  $p_i$  for all categories,  $n_i$  is the total number of stations in category  $i$ , and  $n$  is the total number of stations for all categories. Quotient for mackerel density ( $QD_i$ ) was calculated as:

$$QD_i = \frac{\left(\frac{d_i}{d}\right)}{\left(\frac{p_i}{p}\right)}, \quad (4)$$

where  $d_i$  is the sum of mackerel density in category  $i$ ,  $d$  is the total sum of mackerel density for all categories,  $p_i$  is the total number of stations with mackerel present in category  $i$ , and  $p$  is the

total number of stations with mackerel present for all categories. Confidence intervals (CI) for a random distribution (quotient = 1) were calculated using randomization with replacement, assuming independent observations, with number of values within category remaining the same, and with ten thousand replicas (Bernal et al., 2007). Analysis was done using the “shachar” library (Bernal et al., 2007) in R (version 3.3.0; R Core Team, 2012). Mackerel distribution is not influenced by environmental conditions when the quotient curve is flat and all quotients are not statistically different to one (Bernal et al., 2007).

Generalized additive models (GAM) were used to investigate the multivariate relationship between environmental variables (temperature and mesozooplankton abundance) and SSB on mackerel distribution as such models capture nonlinear relationships (Hastie and Tibshirani, 1990). Multicollinearity of explanatory variables was explored by calculating Pearson correlation coefficient for all possible pairs of explanatory variables. Correlation ranged from -0.54 to 0.30 and collinearity did not demand exclusion of any explanatory variables (Zuur et al., 2009). Geographical location was included as a co-variate to account for its effects. Mackerel frequency of presence ( $P$ ) and density ( $\log_{10}D$ ) were analysed separately using the model (only density model shown as the dependent variables are the same):

$$\log_{10}D_{i,(\lambda, \phi)} = a + s_1[\lambda_i, \phi_i] + s_2[Temp_i] + s_3[\log_{10}Zoo_i] + \beta * SSB + e_i, \quad (5)$$

where  $a$  is the model intercept,  $\lambda$  is longitude,  $\phi$  is latitude at station  $i$ ,  $SSB$  is the estimated mackerel spawning stock biomass with linear coefficient  $\beta$ ,  $s_1$  is a two-dimensional smoothing function,  $s_{2,3}$  are one dimensional smoothing functions for temperature and mesozooplankton, and  $e_i$  is the error term. Furthermore, GAMs were used to explore the effects of environmental variables and stock size on mackerel relative mean weight-at-length ( $WL$ ) using the model:



$$WL_{i,(\lambda, \phi)} = a + s_1[\lambda_i, \phi_i] + s_2[\log_{10}D_i] + s_3[Temp_i] + s_4[\log_{10}Zoo_i] + s_5[DOY_i] + \beta*SSB + e_i, \quad (6)$$

where  $a$  is the model intercept,  $\lambda$  is longitude,  $\phi$  is latitude at station  $i$ ,  $SSB$  is the estimated mackerel spawning stock biomass with linear coefficient  $\beta$ ,  $s_1$  is a two-dimensional smoothing function,  $s_{2-5}$  are one dimensional smoothing functions for the effects of location, mackerel density, environment, and sampling date (day-of-year ( $DOY$ )) on mackerel mean relative weight-at-length ( $WL_i$ ), and  $e_i$  is the model error term. In both equation (5) and (6), stations missing either temperature or mesozooplankton recordings were excluded from analysis. Mesozooplankton dry weight and mackerel density were log transformed to reduce skewness of data before analysis.

The parsimony principle was used to select the best model from all possible combinations of explanatory variables by selecting the model with the lowest Akaike Information Criterion (AIC) (Burnham and Anderson, 2002). If the AIC difference between competing models was  $< 3$ , analysis of variance was used to compare the nested models, accepting the simpler one if the models were not statistically different ( $p < 0.05$ ; Burnham and Anderson, 2002). A non-parametric statistical test was used when model residuals from a parametric model violated assumptions of a normal distribution, homoscedasticity or independence (Zar, 1999). The “mgcv” package (version 1.8-4; Wood, 2006) was used for GAMs and the “Kendall” package (version 2.2; McLeod, 2011) for non-parametric correlation analysis. All statistical analyses were done using R (R Core Team, 2014).

### 3. Results

### 3.1. *Geographical expansion and mackerel density*

The total area occupied by mackerel in Nordic Seas during the summer feeding season, from 1997 to 2016, ranged from 0.4 to 2.5 million km<sup>2</sup>. The smallest area was in 1997, from 1998 to 2006 it was between 0.8 and 1.0 million km<sup>2</sup>, then the expansion began in 2007, peaked in 2014 at 2.5 million km<sup>2</sup>, and declined slightly in the last two years (Fig. 4a). The expansion coincided with a shift in COG and both parameters peaked in 2014 when total area was three-fold larger than the average total area for the period from 1997 to 2006, and COG was located 408 km farther northward and 1650 km farther westward than average COG (Fig. 4b,c; Fig. 2a-h). There was a significant positive correlation between estimated mackerel SSB and both area occupied and shifts in COG (Table 1).

Mackerel occurred at 82% of trawl stations in Nordic Seas, in 2007 and from 2010 to 2016. Occurrence was highest in the traditional feeding area (97%) compared to the northward (78%) and westward (67%) expansion areas, respectively. Mackerel density (i.e. standardized catch rate) among stations with mackerel present ranged from  $4 \times 10^{-4}$  metric ton km<sup>-2</sup> to 60 metric ton km<sup>-2</sup>, with an average of 3.5 metric ton km<sup>-2</sup>, and with a large inter-quartile ranging from ~0.2 to ~6.5 metric ton km<sup>-2</sup> (Fig. 5). Density was highest (median value) in the traditional area, compared to expansion areas, in all years. The year 2011 was excluded from the comparison due to limited coverage in the Norwegian Sea (Fig. 2c). The two expansion areas had similar median density, but the westward area had greater number of high density stations in some years. Annual variability in density differs between areas except there were low values in all areas in 2007 compared to other years. In the traditional area, density increased from 2007 to a peak in 2014 and then declined during the last two years, whereas density peaked in the northward expansion

area in 2012. In the westward area, density remained similar from 2012 to 2016, and was slightly higher than in the earlier years.

### 3.2. *Environmental and SSB effects on expansion*

Sea surface temperature encountered at trawl stations in 2007 and from 2010 to 2016, ranged from  $-0.9^{\circ}\text{C}$  to  $14.8^{\circ}\text{C}$  (Fig. 6a), but mackerel occurrence was limited to temperatures  $\geq 4.8^{\circ}\text{C}$  (Fig. 6a,b). Univariate quotient analyses indicated that mackerel occurrence and density were statistically related to temperature as some of the quotient values were outside the 95% CIs for an even distribution across all temperature categories. Our results suggest that mackerel avoided (occurrence quotient value  $<$  lower 95% CI) areas with temperatures ranging from  $5.0^{\circ}\text{C}$  to  $7.0^{\circ}\text{C}$ , but their presence was possible. Mackerel were present in temperatures ranging from  $7.0^{\circ}\text{C}$  to  $9.0^{\circ}\text{C}$  and from  $13^{\circ}\text{C}$  to  $15^{\circ}\text{C}$ . However, their density was lower than expected for an equal distribution of density across temperature categories (density quotient value  $<$  lower 95% CI). Temperatures ranging from  $9^{\circ}\text{C}$  to  $13^{\circ}\text{C}$  can be considered as the preferred temperature range for mackerel during their summer feeding migration in Nordic Seas, as both their occurrence and their density was either equal to or higher than expected for an equal distribution across temperature categories (quotient value  $>$  lower 95% CI). Mackerel preferred temperature habitat was available both in large parts of the traditional feeding area, in the Norwegian Sea, and in parts of the westward expansion area, which are dominated by warm Atlantic waters (Fig. 7a-h). In contrast, temperature was frequently below preferred values in the northward expansion area.

Mesozooplankton dry weight, from 2010 to 2016, ranged from  $1 \cdot 10^{-3} \text{ g m}^{-2}$  to  $43 \text{ g m}^{-2}$  (Fig. 8a-h) and mackerel occurred in all density categories (Fig. 9a). Univariate quotient analysis of

mesozooplankton indicated that there was no relation between mesozooplankton abundance and mackerel occurrence or density, as all quotients were located within the 95% CIs for an equal mackerel distribution across all mesozooplankton dry weight categories (Fig. 9b).

Results from the multivariate analyses suggested that environmental influences were more complex than indicated by the univariate quotient analysis as the fitted GAMs of both mackerel occurrence and mackerel density contained significant non-linear effects of temperature and mesozooplankton, and positive linear effect of SSB (Fig. 10a-d; Table 2). The fit of univariate GAMs suggested that temperature was the best predictor of mackerel occurrence and density. Mackerel occurrence and density increased with increasing temperatures to 10-11°C, then plateaued or decreased slightly as temperature increased further. Mackerel occurrence increased at mesozooplankton abundance  $> 1 \text{ g m}^{-2}$ , and mackerel density increased for mesozooplankton abundances ranging from  $\sim 1 \text{ g m}^{-2}$  to  $\sim 10 \text{ g m}^{-2}$ . Mackerel density then declined as mesozooplankton increased further. At mesozooplankton abundance below  $1 \text{ g m}^{-2}$ , no conclusions could be drawn as there were too few samples and wide confidence intervals (CI) on the fitted values. The best GAMs explained 47.0% and 31.8% of the variation in mackerel occurrence and mackerel density, respectively (Table 2). The GAM results were visually explored for spatial autocorrelation. There was a weak spatial pattern in model residuals for mackerel occurrence (Fig. S1a; supplementary material provided online), with location of negative values mirroring distribution pattern of zero catch stations. No pattern was observed in model residuals for mackerel density (Fig. S1b).

The best model for mackerel density predicted major spatial trends in the Norwegian Sea and in the westward expansion area, when the spatial grid was expanded to cover a grid of the Northeast Atlantic (Fig. 11; Fig. S2).

### 3.3. *Temperature trends and geographical distribution*

From 1997 to 2016, the remotely sensed average monthly SST, from May to July, was significantly colder in the northward expansion area compared to the westward area (Fig. 12a-b). The monthly average SST increased by approximately 3.5°C from May to July. In the westward area, monthly averages ranged from 6.2°C to 11.3°C and was warm enough for high mackerel density in July ( $> 9^{\circ}\text{C}$ ) in all years, whereas June values were warm enough for high mackerel density in eight of the twenty years and sufficed for low mackerel density ( $7^{\circ}\text{C} - 9^{\circ}\text{C}$ ) in the other years. During May temperature was warm enough for low mackerel density in half the years, but too cold for mackerel during the other ten years ( $< 5^{\circ}\text{C}$ ). In the northward area, average temperature ranged from 3.2°C to 9.1°C, which was below preferred temperatures for high density of mackerel, with one exception in July 2014. However, it was warm enough for low mackerel density in July and mackerel presence was possible in June ( $5^{\circ}\text{C} - 7^{\circ}\text{C}$ ) but unlikely in May ( $< 5^{\circ}\text{C}$ ).

SST shifted above the long-term average in 2003 and 2007 lasting two years and four years, respectively. From 2011 to 2016, SST fluctuated between low and high values in the westward area, whereas temperatures in the northward area followed a similar temporal change but the amplitude of variability was smaller.

### 3.4. *Cumulative feeding success and its geographical variation*

Mackerel relative mean weight-at-length calculated as average per station in 2007 and from 2010 to 2016 ranged from -129 g to +124 g (Fig. 13). Weight-at-length was highest in 2007, then declined until 2012 and remained similar for the remaining years except for a slight increase in 2014. Annual variation followed a similar pattern in all areas. When comparing areas within each year, weight-at-length was highest in the westward expansion area and lowest in the traditional feeding area, in most years.

The fit of univariate GAMs suggested mackerel density was the best indicator of mackerel relative mean weight-at-length (Table 3). The best GAM model for weight-at-length included DOY, temperature, mackerel density, and SSB, and explained 44.5% of the variance (Fig. 14a-c). Weight-at-length was positively influenced by temperature. DOY relationship with weight-at-length was linear for the month of July to middle of August (DOY ~230) which includes the majority of observations. Mackerel density had a positive effect on weight-at-length and is the relationship best described by a logistic curve. SSB had a positive linear effect on weight-at-length. There was no spatial pattern in residuals of the best GAM (Fig. S1c). A model also including mesozooplankton abundance was significantly worse (ANOVA:  $p = 0.348$ ).

When the best GAM model was expanded to cover a grid of the Northeast Atlantic, it predicted a contour of positive mackerel weight-at-length stretching from the northern part of the traditional feeding grounds towards the east coast of Iceland, westward along Iceland south coast, and towards the east coast of Greenland (Fig. 15). It captured major spatial trends in the observed relative weight-at-length, which were similar in all the years (Fig. S3).

## 4. Discussion

#### 4.1. *Temperature effect*

Temperature directly constrained mackerel geographical distribution during the summer feeding season in the Nordic Seas during the expansion period from 2007 to 2016. Mackerel prefer temperatures ranging from 9° to 13°C and where temperatures in the expanded areas were within that range resulted in both high mackerel presence and high mackerel density. Mackerel also occupied waters with temperatures ranging from 7° to 9°C, although in this range while mackerel presence was still high, their density was low. They also tolerated temperatures between 5° to 7°C, but in these waters both mackerel presence and density were low. Mackerel avoided waters colder than 5°C. To our knowledge, this was the first time mackerel temperature preference was quantified during their summer feeding migration in the Nordic Seas. Other studies have approximated the temperature occupied by mackerel as ranging from 8°C to 14°C, which was supported by our results (Iversen, 2002; Utne et al., 2012, Jansen et al., 2016, Nøttestad et al., 2016b).

During the period from 2007 to 2016 mackerel expanded their distribution into preferred, acceptable, and tolerable thermal habitats located adjacent to their traditional feeding grounds in the Norwegian Sea. It appears mackerel reached the northward boundary of their available thermal habitat in the Norwegian Sea (east of longitude 10°W), as waters in the northward expansion area were mostly acceptable, in part tolerable but not preferred. In contrast, preferred temperatures dominated large parts of the westward expansion area (west of longitude 10°W), which was a virgin habitat for mackerel prior to the beginning of expansion in 2007. Two different surface currents dominate the westward area, cold Polar waters north of Iceland and warm Atlantic waters to the south. Cold Polar waters ( $< \sim 5^{\circ}\text{C}$ ; Blindheim and Østerhus, 2005)

prevented mackerel from expanding northwestward into the Iceland Sea and the Greenland Sea thus constraining the westward movement of mackerel to the Irminger current along the south coast of Iceland and south-westwards into Greenlandic waters.

The mackerel expansion from 2007 onward cannot be explained by sudden changes in temperature from values below preferred range to values within preferred range. This agrees with Astthorsson et al. (2012) results that the initiation of mackerel westward expansion was not concurrent with sudden temperature changes in Icelandic waters, however they concluded that long-term changes in temperature contributed to westward expansion of mackerel. This applies both to temperatures during the peak of the feeding season in July and in the earlier phase of the migration in May and June. According to old records, surface currents south and west of Iceland have been within mackerel preferred temperature range from June to September since at least 1832 (Hanna et al., 2006). However, temperature influences on a fish stocks geographical distribution are not limited to direct constraints. Even small changes in temperature ( $< \sim 2^{\circ}\text{C}$ ) can influence stock distribution on various temporal and spatial scales (Drinkwater, 2003, 2006; Sundby and Nakken, 2008). Temperature changes often coincide with large-scale changes in circulation patterns, nutrient upwelling and plankton production, which are likely to influence prey availability of pelagic plankton feeders like mackerel (Nye et al. 2014; Hátún et al. 2016; Pacariz et al., 2016). Astthorsson et al. (2012) split the period from 1880 to 2012 into five temperature regimes of alternating warm, cold and intermediate surface waters. The current period is warm and began in 1996. The current warm period does not coincide with higher mesozooplankton densities compared to the prior intermediate temperature period, from 1970 to 1996 (Figure 15b in Marine and Freshwater Research in Iceland, 2016).

Temperature cannot explain the lack of mackerel presence in the Iceland Basin (see Fig. 1) as it is within the preferred range. Pacariz et al. (2016) suggested that nutrient-depletion limits



zooplankton production in the Iceland Basin during summer and that confines mackerel westward movement to a corridor on the shelf south of Iceland. Absence of mackerel and low mesozooplankton densities in the Iceland Basin measured by IESSNS from 2010 to 2016 support this hypothesis except for 2015. However, in 2015, the Iceland Basin was surveyed in the first week of July compared to the last week of July in the other years. Stratification of the surface mixed layer limits nutrients enrichment of the layer after the initial spring bloom causing nutrients to decline from May to August (Pacariz et al., 2016). This approximately three-week difference in survey dates could explain why mackerel abundance and mesozooplankton density was high in the Iceland Basin in 2015 compared to the other years. Pacariz et al. (2016) furthermore suggested that the ongoing nutrient decline throughout the subpolar North Atlantic (Hátún et al., 2017a; Rey, 2012), together with the west-east (high-low) horizontal nutrient gradient, might have added to the density-dependent depletion of food resources in the east, forcing mackerel to migrate farther north and west in their search for food.

#### 4.2. *Prey abundance*

The GAM results indicated that mesozooplankton abundance influenced mackerel occurrence and mackerel density. Mackerel distribution expansion resulted in occupancy of new areas with high mesozooplankton abundance. The seasonal development of mesozooplankton in the Norwegian Sea and adjacent areas is delayed towards west and north (Broms and Melle, 2007; Bagøien et al., 2012), and the mackerel expansion areas westward and northward of the traditional feeding area, may offer good feeding conditions later in the feeding season compared to the traditional area. Mackerel may follow gradients of increasing prey abundance into the

western and northern areas, as suggested to be a navigation mechanism of herring feeding migration in a partly overlapping area (Broms et al., 2012). The expansion northward into a thermal habitat below their preferred range ( $<9^{\circ}\text{C}$ ) may be a trade-off between temperature preferences and prey availability as well as prey quality. The mackerel undertakes this extensive feeding migration during summer to accumulate energy reserves for the subsequent overwintering and spawning season (Olafsdottir et al., 2016, Bachiller et al., 2018). However, the feeding migration does not expand into the Iceland and Greenland Seas (Fig. 1), even though these areas have high mesozooplankton abundance, due to intolerably low temperatures ( $<\sim 5^{\circ}\text{C}$ ; Fig. 7).

The GAM results for relative mean weight-at-length did not include positive effects of mesozooplankton abundance but of mackerel density. Positive effects of mackerel density suggested that during the feeding season mackerel aggregated in response to prey abundance. This predicts that areas of high productivity attracted greater densities of mackerel, which is supported by the positive relationship between mackerel occurrence/density and mesozooplankton densities. Therefore, it is surprising that mesozooplankton density did not have a significant positive effect on relative mean weight-at-length. There are several possible explanations for this. Individuals feeding in areas with a lot of prey could gain more weight and reduce mesozooplankton abundance levels, which might prevent observations of a positive relationship. Variability in prey abundance experienced earlier in the feeding season could contribute as mesozooplankton densities have a large temporal variation within the annual summer feeding period (Melle et al., 2004; Astthorsson and Gislason, 2003). Temporal variation in prey quality, i.e. energy content, could also contribute (Rand et al., 2010). Mackerel prey on a wide size range of prey items (Prokopchuk and Sentyabov, 2006; Langøy et al., 2012; Óskarsson et al., 2016; Bachiller, et al., 2016) of which the larger prey is poorly sampled with WP2-nets

(Gjøsæter et al., 2000). Larger prey items constitute anywhere from none to ~ 85 % of total stomach content (Langøy et al., 2012; Óskarsson et al., 2016; Bachiller et al., 2018). Availability of larger prey is likely to influence cumulative feeding success, but their importance cannot be estimated as the necessary data on abundance of larger prey items is not available. We cannot evaluate the potential importance of these factors. However, it is obvious that mesozooplankton density (collected using WP2-nets) measured concurrently with mackerel sampling is not reflective of feeding success experienced during the feeding season.

Other factors in combination with mesozooplankton production could influence mackerel relative mean weight-at-length during the feeding season, such as interspecific competition (Utne et al., 2012; Huse et al., 2012). Norwegian spring-spawning herring (*Clupea harengus*) is a major competitor, as they feed on the same main prey items as mackerel, while blue whiting (*Micromesistius poutassou*) is a minor competitor with smaller overlap in diet (Langøy et al., 2012). Previous studies indicate that herring and blue whiting stock size negatively influence mackerel cumulative feeding success (Huse et al., 2012; Olafsdottir et al., 2016). From 2010 to 2016, herring SSB declined ~ 40% and blue whiting SSB increased ~30% (ICES, 2016). It is likely that declining competition from herring contributed to higher mackerel feeding success and offset the increasing competition from blue whiting.

It appears that the feeding season peaked in the middle of August. At that time DOY effects on cumulative feeding success shifted from positive to negative. This supports Bachiller et al. (2018) and Olafsdottir et al. (2016) conclusion that mackerel annual feeding season peaks in August. However, in the present study only 3% of stations were collected in the latter half of August and these stations were limited to 2010 and 2011. Given the small sample size and limited number of years, the negative DOY effects should be interpreted with caution.

### 4.3. Stock size effect

Several of our results suggest that the observed mackerel summer feeding range expansion from 2007 to 2016 is a density dependent response to increasing stock size as predicted by MacCall's basin model (MacCall, 1990). When SSB increased, distribution range increased concurrently with increasing mackerel density. Mackerel density appeared higher on the traditional feeding grounds compared to expansion areas. There was spatial variation in mackerel relative weight-at-length, but it was neither associated with the traditional feeding grounds nor expansion areas. Instead high and low relative mean weight-at-length were present both on the traditional feeding grounds and in expansion areas.

Surprisingly, SSB positively affected mackerel relative mean weight-at-length. This is theoretically possible as there is a large annual variability in productivity of Nordic Seas (Astthorsson and Gislason, 2003; Melle et al., 2004). Measured mean annual mesozooplankton biomass in spring in the Norwegian Sea and in Atlantic waters in the Icelandic EEZ, ranges approximately from 1 to 30 g dry weight  $\text{m}^{-2}$  (Figure 15 in Marine and Freshwater Research in Iceland, 2016; Melle et al., 2004). The data needed to measure mackerel cumulative prey availability from beginning of the feeding season (May/June) until capture (July/August) do not exist. The only data available to us are mesozooplankton abundance at time of sampling. There was no correlation between mean annual mesozooplankton densities and SSB (IESSNS data from 2010 to 2016, Kendall correlation test,  $\tau = 0.43$ ,  $p = 0.27$ ,  $n = 7$ ). This supports our previous conclusion (section 4.2) that mesozooplankton abundance measured during IESSNS is not a suitable index for mackerel relative mean weight-at-length at the time of sampling. For mesozooplankton abundance, measured once during the feeding season, to be a useful index for

annual mesozooplankton production, the production rate must be constant during the feeding season, and this is certainly not the case (Astthorsson and Gislason, 2003; Melle et al., 2004).

Surprisingly, SSB positively influenced mackerel relative mean weight-at-length. Several factors could have contributed to the positive SSB effects, such as annual variation in ecosystem productivity, and that mackerel westward and northward expansion more than compensated for increasing SSB, facilitating greater feeding success in years with higher SSB. However, it contradicted the conclusion of negative effects by Olafsdottir et al. (2016). This could be explained by analytical differences as Olafsdottir et al. (2016) analysed individuals weight-at-length at the end of seasonal feeding season, September and October, compared to relative mean weight-at-length in the middle of the feeding season used in the current paper. Olafsdottir et al. (2016) results showed that density effects were more pronounced for larger ( $> 35$  cm) individuals than smaller ones. The mean relative weight-at-length merges individuals of all sizes into one value per station, hence ignores length variability in weight gain. Another explanation is how short the present study period was, only seven years compared to three decades in Olafsdottir et al. (2016). It is possible that during the longer period there were years when low productivity and high SSB concurred. Furthermore, interspecific competition with herring and blue whiting was probably different during the long period compared to our study. In the long period, both herring and blue whiting SSB changed respectively by a factor of 2.5 and 3.5 (ICES, 2016). Likely a combination of different analytical methods, annual differences in mesozooplankton production, mackerel geographical distribution and in interspecific competition for prey contributed to different conclusions between the two study periods.

In 2015 and 2016, mackerel SSB declined from the peak in 2014 (ICES, 2016) and concurrently the area occupied declined and COG shifted southward and eastward. Given the present knowledge, it is impossible to predict if the current expansion areas will be abandoned

when stock size declines to low levels of the pre-expansion period as more factors besides stock size, temperature, and feeding condition influence the mackerel distribution. Migration distance and collective memory of the migration route and spawning site fidelity are factors that could influence future distribution (Fernö et al., 1998; Corten, 2002). Research on distribution change of herring in relation to stock size indicate that cohorts tend to visit the same feeding grounds for the duration of their lives, and that new feeding grounds become occupied when large cohorts are recruited to the feeding migration (Corten, 2002; Huse et al., 2002). We suggest that periphery areas in the northward and the westward expansion areas are likely to be abandoned first if stock size keeps declining due to long migration distance. However, it is impossible to predict whether mackerel will retract to the central and eastern core areas with declining stock size.

Changes in age- and size-structure of the mackerel stock could contribute to variability in distribution range as larger individuals are known to migrate further westward and northward compared to smaller individuals (Nøttestad et al., 2007, 2010 - 2015, 2016b, 2016c). Mackerel length-at-age has declined from mid-2000s to 2013 (Olafsdottir et al., 2013) and no drastic changes in age structure of the stock have occurred (ICES, 2016). It is possible that declining length-at-age reduced the distribution expansion, however evaluation of such effects is outside the scope of the current paper.

Our results represent how temperature and to a lesser degree mesozooplankton abundance constrained mackerel summer feeding distribution in Nordic Seas during the last decade as SSB doubled. This does not eliminate potential effects of multidecadal changes in marine climate, nutrient concentrations, primary and secondary production on the observed distribution expansion. A warm climate phase in the North Atlantic has been correlated to increasing populations size and geographical distribution changes in many fish populations on multidecadal time scale (Drinkwater et al., 2003, 2006; Astthorsson et al., 2007; Sundby and Nakken, 2008).

The current warm period in the North Atlantic began approximately a decade prior to mackerel geographical expansion (González-Pola et al., 2018). This warming that began in the mid-1990s might have contributed to favourable condition on the spawning grounds and the nursing ground that resulted in several large cohorts from 2002 to 2014 compared to few from 1980 to 2002 (ICES, 2016). The mechanism explaining the high frequency of large year classes in the last decade is not yet fully understood, however importance of copepodites abundance on the nursing grounds has been identified (Jansen, 2016). The increase in SSB in the mid-2000s, as a result of the strong 2002 cohort entering the spawning stock, concurred with the beginning of the summer feeding distribution expansion. It is possible that expanding distribution feedback into increasing SSB mediated via changes in growth, reproduction, recruitment and mortality rate. It has proven elusive to identify the operational mechanism of how changes in marine climate influence ecology of fish stocks (Drinkwater et al., 2010). Hence, it is likely that the observed mackerel summer distribution expansion observed from mid-2000s onward is caused by a combination of many factors, and their feedback on each other, operating on various temporal scales.

## 5. Conclusions

Our results suggested that mackerel geographical expansion during the summer feeding season in the Nordic Seas, from 2007 to 2016, was primarily driven by an increasing mackerel stock size and constrained by availability of preferred temperature habitat. This facilitated mackerel expansion into two major directions, COG shifted northward within the Norwegian Sea towards Svalbard by approximately 400 km, and westward by approximately 1650 km along the Irminger current south of Iceland and into Greenland waters, compared to the period from 1997

to 2006. Intolerably cold waters ( $< 5^{\circ}\text{C}$ ) prevented mackerel from expanding into the Iceland Sea and the Greenland Sea, as well as into areas west and northwest of Jan Mayen. Spatial variability in mackerel relative mean weight-at-length suggested that mackerel expanded into areas that offered similar feeding habitat, to the traditional feeding grounds. It appears that as stock size increased a suitable feeding habitat located adjacent to the traditional feeding grounds became inhabited by mackerel. Multidecadal changes in marine climate are likely to have contributed to the observed distribution expansion but are not evaluated in the current paper. Our results are limited to the direct effects of temperature, mesozooplankton abundance, and SSB on distribution range during the last two decades.

## 6. Acknowledgements

We thank the crewmembers participating in the many scientific surveys on research vessels and chartered fishing vessels, which provided the data for our study and were conducted by: Institute of Marine Research, Norway, Marine Research Institute, Iceland, the Faroe Marine Research Institute, Faroe Island, and Greenland Institute of Natural Resources, Greenland. We are grateful to the ICES Working Group on Widely Distributed Stocks and to NOAA/OAR/ESRL PSD, Boulder, CO, USA, for making available SST data and estimates on mackerel stock size. We are indebted to Sigurður Þór Jónsson, Marine Research Institute, Reykjavik, Iceland, Dr. Christoph Konrad, Centre for Fisheries Ecosystem Research, Memorial University, St. John's, Canada, and Joshua Mark Lawrence, School of Biological Sciences, University of Aberdeen, Aberdeen, Scotland, for assistance with modelling. Finally, we thank the two reviewers and the editor for their constructive comments which greatly improved the paper. Majority of A.H.O.



work was funded by the Danish government through the program “Marine climate in the North Atlantic and its effects on plankton and fish”. The funding source was not involved in study design, data collection, analysis, and interpretation, writing of the manuscript or in the decision to submit the article for publication.

Accepted manuscript

## References

- Astthorsson, O. S. and Gislason, A. 2003. Seasonal variations in abundance, development and vertical distribution of *Calanus finmarchicus*, *C. hyperboreus* and *C. glacialis* in the East Icelandic Current. *Journal of Plankton Research*, 25: 843–854.
- Astthorsson, O. S., Gislason, A., and Jonsson, S. 2007. Climate variability and the Icelandic marine ecosystem. *Deep Sea Research II*, 54: 2456–2477.
- Astthorsson, O. S., Valdimarsson, H., Gudmundsdottir, A., and Óskarsson, G. J. 2012. Climate-related variations in the occurrence and distribution of mackerel (*Scomber scombrus*) in Icelandic waters. *ICES Journal of Marine Science*, 69: 1289–1297.
- Bachillier, E., Skaret, G., Nøttestad, L., and Slotte, A. 2016. Feeding ecology of Northeast Atlantic mackerel, Norwegians spring-spawning herring and blue whiting in the Norwegian Sea. *PLoS ONE* 11(2):e0149238. Doi:10.1371/journal.pone.0149238.
- Bachiller E., Utne K. R., Jansen T., and Huse G. 2018. Bioenergetics modeling of the annual consumption of zooplankton by pelagic fish feeding in the Northeast Atlantic. *PLOS ONE* 13(1): e0190345. <https://doi.org/10.1371/journal.pone.0190345>
- Bagøien, E., Melle, W., Kaartvedt, S. 2012. Seasonal development of mixed layer depths, nutrients, chlorophyll, and *Calanus finmarchicus* in the Norwegian Sea – A basin scale habitat comparison. *Progress in Oceanography*, 103: 58-79.
- Barange, M., Coetzee, J., Takasuka, A., Hill, K., Gutierrez, M., Oozeki, Y., van der Lingen, C. *et al.* 2009. Habitat expansion and contraction in anchovy and sardine populations. *Progress in Oceanography*, 83: 251–260.
- Belikov, S. V., Jakupsstovu, S. H., Shamrai, E., and Thomsen, B. 1998. Migration of mackerel during summer in the Norwegian Sea. *ICES CM/AA8*: 1–14.
- Berge, J. Heggland, K., Lønne, O. J., Cottier, F., Hop, H., Gabrielsen, G. W., Nøttestad, L., Misund, O. A. 2015. First Records of Atlantic Mackerel (*Scomber scombrus*) from the Svalbard Archipelago, Norway, with Possible Explanations for the Extension of Its Distribution. *Arctic* 68(1):54-61. DOI:10.14430/arctic4455
- Bernal, M., Stratoudakis, Y., Coombe, S., Angelico, M. M., Lago de Lanzós, A., Porteiro, C., Sagarminaga, Y. *et al.* 2007. Sardine off the European Atlantic coast: Characterization of and spatio-temporal variability in spawning habitat. *Progress in Oceanography* 74: 210–227.
- Bjornsson, H., Jonsson, S. T., Magnusson, A. and Elvarsson, B. T. 2015. geo: Draw and Annotate Maps, Especially Charts of the North Atlantic. R package version 1.4-3. <http://CRAN.R-project.org/package=geo>.

- Blindheim, J., and Østerhus, S. 2005. The Nordic Seas, main oceanographic features. In: The Nordic Seas: An Integrated Perspective. Oceanography, Climatology, Biogeochemistry, and Modeling. Geophysical Monograph Series, 158. H. Drange, T., Dokken, T. Furevik, R. Gerdes and W. Berger (eds). Washington, DC: AGU, 11-37. doi:10.1029/158GM03.
- Brett, J. R. 1979. Environmental factors and growth. In: Hoar, W. S., Randall, D. J., Brett, J. R. (eds) Bioenergetics and growth, Vol. 8. Academic Press, New York, p 599-667.
- Broms, C., and Melle, W. 2007. Seasonal development of *Calanus finmarchicus* in relation to phytoplankton bloom dynamics in the Norwegian Sea. Deep-Sea Research II 54: 2760–2775.
- Broms, C., Melle, W., and Horne, J. K. 2012. Navigation mechanisms of herring during feeding migration: the role of ecological gradients on an oceanic scale. Marine Biology research, 8: 461–474.
- Burnham, K. P., and Anderson, D. R. 2002. Model Selection and Multimodel Inference: A Practical Information-Theoretic Approach. Springer-Verlag, New York. 488 pp.
- Corten, A. 2002. The role of “conservatism” in herring migrations. Reviews in Fish Biology and Fisheries, 11: 339–361.
- Dragesund, O., Johannessen, A., and Ulltang, Ø. 1997. Variation in migration and abundance of Norwegian spring-spawning herring (*Clupea harengus* L.). Sarsia, 82: 97–105.
- Drinkwater, K. F. 2006. The regime shift of the 1920s and 1930s in the North Atlantic. Progress in Oceanography, 68: 134–151.
- Drinkwater, K. F., Belgrano A., Borja, A., Conversi, A., Edwards, M., Greene, C. H., Ottersen, G. et al. 2003. The response of marine ecosystems to climate variability associated with the North Atlantic Oscillation. In The North Atlantic Oscillation: climatic significance and environmental impact, 134, pp 211–234. Ed. by J. W. Hurrell, Y. Kushnir, G. Ottersen, and M. Visbeck, M. American Geophysical Union, Washington, DC. 279 pp.
- Drinkwater, K. F., Beaugrand, G., Kaeriyama, M., Kim, S. Ottersen, G., Perry, R. I., Pörtner, H.-O., et al. 2010. On the process of linking climate to ecosystem changes. Journal of Marine Systems, 79: 374–388.
- Drinkwater, K. F., Miles, M., Medhaug, I., Otterå, O. H., Kristiansen, T., Sundby, S., and Gao, Y. 2014. The Atlantic Multidecadal Oscillation: Its manifestations and impacts with special emphasis on the Atlantic region north of 60 °N. Journal of Marine Systems 133: 117-130.
- Fernö, A., T. J. Pitcher, V. Melle, L. Nøttestad, S. Mackinson, C. Hollingworth and O.A. Misund 1998. The challenge of the herring: Making optimal collective spatial decisions. Sarsia 83:149–167.

- Frank, K. T., Carscadden, J. E., and Simon, J. E. 1996. Recent excursions of capelin to the Scotian Shelf and Flemish Cap during anomalous hydrographical conditions. *Canadian Journal of Fisheries and Aquatic Sciences*, 53: 1473–1486.
- Fretwell, S. D. and Lucas, H.L. 1969. On territorial behavior and other factors influencing habitat distribution in birds. I. Theoretical development. *Acta Biotheor* 1:16–36.
- Gislason, A. 2003. Life-cycle strategies and seasonal migrations of oceanic copepods in the Irminger Sea. *Hydrobiologia*, 503: 195–203.
- Gisslason, A. 2008. Vertical distribution and seasonal dynamics of mesozooplankton in the Iceland Basin. *Marine Biology Research*, 4: 401–413.
- Gislason, A., and Astthorsson, O. S. 1995. Seasonal cycle of zooplankton southwest of Iceland. *Journal of Plankton Research*, 17: 1959–1976.
- Gislason, A., and Astthorsson, O. S. 2004. Distribution patterns of zooplankton communities around Iceland in spring. *Sarsia*, 89: 467–477.
- Gjøsæter, H., Dalpadado, P., Hassel, A. And Skjoldal, H. R. 2000. A comparison of performance of WP2 and MOCKNESS. *Journal of Plankton Research*, 22: 1901–1908.
- González-Pola, C., Larsen, K. M. H., Fratantoni, P., Beszczynska-Möller, A., and Hughes, S. L. (Eds). 2018. ICES Report on Ocean Climate 2016. ICES Cooperative Research Report No. 339. 110 pp. <https://doi.org/10.17895/ices.pub.4069>
- Gødo, O. R., Hjellvik, V., Iversen, S. A., Slotte, A., Tenningen, E., and Torkelsen, T. 2004. Behavior of mackerel schools during summer feeding migration in the Norwegian Sea, as observed from fishing vessel sonars. *ICES Journal of Marine Science*, 61: 1093–1099.
- Häkkinen, S. and Rhines, P. B. 2004. Decline of subpolar North Atlantic circulation during the 1990s. *Science*, 304: 555–559.
- Hanna, E., Jonsson, T., Olafsson, J., and Valdimarsson, H. 2006. Icelandic coastal sea surface temperature records constructed: putting the pulse on air-sea-climate interactions in the northern North Atlantic. 1. Comparison with HadISST1 open ocean surface temperatures and preliminary analysis of long-term patterns and anomalies of SST around Iceland. *Journal of Climate*, 19: 5652–5666.
- Hansen, F. T., Burns, F., Post, S., Thygesen, U. H., and Jansen, T., 2018. Length measurement methods of Atlantic mackerel (*Scomber scombrus*) and Atlantic horse mackerel (*Trachurus trachurus*) – current practice, conversion keys and recommendations. *Fisheries Research*, 205: 57–64.
- Hastie, T. J., and Tibshirani, R. J. 1990. Generalized additive models. Chapman & Hall/CRC Monographs on Statistics and Applied Probability 43. 352 pp.

- Hatun, H., Sando, A. B., Drange, H., Hansen, B., and Valdimarsson, H. 2005. Influence of the Atlantic subpolar gyre on the thermohaline circulation. *Science*, 309: 1841–1844.
- Hátún, H., Payne, M. R., and Jacobsen, J. A. 2009. The North Atlantic subpolar gyre regulates the spawning distribution of blue whiting (*Micromesistius poutassou*). *Canadian Journal of Fisheries and Aquatic Science*, 66: 759–777.
- Hátún, H., Lohmann, K., Matei, D., Jungclauss, J. H., Pacariz, S., Bersch, M., Gislason, Á. Et al. 2016. An inflated subpolar gyre blows life toward the northeastern Atlantic. *Progress in Oceanography*, 147: 49–66.
- Hátún, H., Azetsu-Scott, K., Somavilla, R., Rey, F., Johnson, C., Mathis, M., Mikolajewicz, U., et al. 2017a. The subpolar gyre regulates silicate concentrations in the North Atlantic. *Scientific Reports* 7. Doi:10.1038/s41598-017-14837-4
- Hátún, H., Olsen, B., and Pacariz, S. 2017b. The Dynamics of the North Atlantic subpolar gyre introduces predictability to the breeding success of kittiwakes. *Frontiers in Marine Science*, 4: 132. Doi: 10.3389/fmars.2017.00123
- Hurrell, J. W. 1995. Decadal trends in the North Atlantic Oscillation: regional temperatures and precipitation. *Science*, 269:676– 679.
- Huse, G., Holst, J. C. , Utne, K., Nøttestad, L., Melle, W. , Slotte, A., Ottersen, G., *et al.* 2012. Effects of interactions between fish populations on ecosystem dynamics in the Norwegian Sea – results of the INFERNO project. *Marine Biology Research*, 8: 415–419.
- Huse, G., Railsback, S., and Fernö, A. 2002. Modelling changes in migration pattern of herring: collective behaviour and numerical domination. *Journal of Fish Biology*, 60: 571–582.
- ICES. 2013. Report of the Ad hoc Group on the Distribution and Migration of Northeast Atlantic Mackerel (AGDMM), Dares, ICES Headquarters, Copenhagen. ICES CM 2013/ACOM:58. 211 pp.
- ICES. 2015. Manual for International Pelagic Surveys (IPS). Series of ICES Survey Protocols SISP 9 – IPS. 92 pp.
- ICES. 2016. Report of the Working Group on Widely Distributed Stocks (WGWISE), 31 August - 6 September 2016, ICES HQ, Copenhagen, Denmark. ICES CM 2016/ACOM:16. 500 pp.
- Iversen, S. A. 2002. Changes in the perception of the migration patterns of Northeast Atlantic mackerel during the last 100 years. *ICES Marine Science Symposia*, 215: 382–390.
- Jakob, E. M., Marshall, S. D., and Uetz, G. W. 1996. Estimating weight-at-length: A Comparison of Body Condition Indices. *Oikos*, 77: 61–67.
- Jansen, T. 2016. First-year survival of North East Atlantic mackerel (*Scomber scombrus*) from

1998 to 2012 appears to be driven by availability of *Calanus*, a preferred copepod prey. Fisheries Oceanography, 25: 457–469.

- Jansen, T., and Burns, F., 2015. Density dependent growth changes through juvenile and early adult life of North East Atlantic mackerel (*Scomber scombrus*). Fisheries Research, 169: 37–44.
- Jansen, T., Campbell, A., Kelly, C. J., Hátún, H., and Payne, M. 2012. Migration and Fisheries of North East Atlantic Mackerel (*Scomber scombrus*) in Autumn and Winter. PLoS One, 7: 1–9.
- Jansen T., Kristensen K., van der Kooij, J. Post, S., Campbell, A., Utne, K. R., Carrera, P., *et al.* 2015. Nursery areas and recruitment variation of North East Atlantic mackerel (*Scomber scombrus*). ICES Journal of Marine Science, 72: 1779–1789.
- Jansen, T., Post, S., Kristiansen, T., Óskarsson, G. J., Boje, J., MacKenzie, B. R., Broberg, M. *et al.* 2016. Ocean warming expands habitat of a rich natural resource and benefits a national economy. Ecological Applications. Accepted Author Manuscript. doi:10.1002/eap.1384
- Langøy, H., Nøttestad, L., Skaret, G., Broms, C., and Fernø, A. 2012. Overlap in distribution and diets of Atlantic mackerel (*Scomber scombrus*), Norwegian spring-spawning herring (*Clupea harengus*) and blue whiting (*Micromesistius poutassou*) in the Norwegian Sea during late summer. Marine Biology Research, 8: 442–460.
- Lluch-Belda, D., Crawford, R. J. M., Kawasaks, T., MacCall, A. D., Parrishs, R. H., Schwartzlose, R. A., and Smith, P. E. 1989. World-wide fluctuations of sardine and anchovy stocks: the regime problem. South African Journal of Marine Science, 8: 195–205.
- Lluch-Belda, D., Lluch-Cota, D. B., Hernández-Vazquez, S., Salinas-Zavala, C., and Schwartzlose, R. 1991. Sardine and anchovy spawning as related to temperature and upwelling in the California Current system. California Cooperative Oceanic Fisheries Investigation Report, 32: 105–111.
- Lockwood, S. J. 1988. The mackerel: its biology, assessment and the management of a fishery. Fishing News Books Ltd, Farnham, Surrey, England. 181 pp.
- MacCall, A. D. 1990. Dynamic geography of marine fish populations. Washington Sea Grant, Seattle. 153 pp.
- Marine and Freshwater Research in Iceland. 2016. Environmental condition in Icelandic waters in 2015. HAV 2016-001. 46pp.
- Marine Research Institute. 2015. State of Marine Stocks in Icelandic Waters 2014/2015 and Prospects for the Quota Year 2015/2016. Marine Research in Iceland 182. 217 pp.
- McLeod, A.I. 2011. Kendall: Kendall rand correlation and Mann-Kendall trend test. R package version 2.2. <http://CRAN.R-project.org/package=Kendall>.

- Melle, W., Ellertsen, B., Skjoldal, H.R., 2004. Zooplankton: the link to higher trophic levels. In: Skjoldal, H.R. (Ed.), *The Norwegian Sea Ecosystem*. Tapir, Trondheim, pp. 137–202.
- Nye, J. A., Baker, M. R., Bell, R., Kenny, A., Kilbourne, K. H., Friedland, K. D., Martino, E., et al. 2014. Ecosystem effects of the Atlantic Multidecadal Oscillation. *Journal of Marine Systems*, 133: 103–116.
- Nøttestad, L., Patel, R., Anthonypillai, V., Langøy, H., Nilson, G., Langard, L., Andersen, J., et al. 2007. Cruise Report on Coordinated Ecosystem Survey with M/V “Libas” and M/V “Eros” in the Norwegian Sea, 15 July–6 August 2007. Unpublished Cruise Report of Institute of Marine Research, Bergen, Norway. 39 pp.
- Nøttestad, L., Patel, R., Anthonypillai, V., Tangen, Ø., Henriksen, I., Wennevik, V., Ellertsen, B., et al. 2009. Cruise report from the coordinated ecosystem survey and SALSEA salmon project with M/V “Libas” and M/V “Eros” in the Norwegian Sea, 15 July– 6 August 2009. Unpublished cruise report from Institute of Marine Research, Bergen, Norway. 60 pp.
- Nøttestad, L., Jacobsen, J. A., and Sveinbjørnsson, S. 2010. Cruise Report from the Coordinated Ecosystem Survey with M/V “Libas”, M/V “Brennholm”, M/V “Finnur Friði” and R/V “Arni Fridriksson” in the Norwegian Sea and Surrounding Waters, 9 July–20 August 2010. Working Document to Working Group of Widely Distributed Stocks, ICES, Copenhagen, Denmark, 28 August– 3 September 2010. 48 pp.
- Nøttestad, L., Holst, J. C., Utne, K. R., Tangen, Ø., Anthonypillai, A., Skalevik, A., Mork, K. A., et al. 2011. Cruise Report from the Coordinated Ecosystem Survey (IESSNS) with M/V “Libas”, M/V “Finnur Friði” and R/V “Arni Fridriksson” in the Norwegian Sea and Surrounding Waters, 18 July–31 August, 2011. Working Document to Working Group of Widely Distributed Stocks, ICES, Copenhagen, Denmark, 27 August–2 September 2011. 31 pp.
- Nøttestad, L., Utne, K. R., Anthonypillai, V., Tangen, Ø., Valdemarsen, J. W., Oskarsson, G., Sveinbjørnsson, S., et al. 2012. Cruise Report from the Coordinated Ecosystem Survey (IESSNS) with R/V “G.O. Sars”, M/V “Brennholm”, M/V “Christian í Grótinum” and R/V “Arni Fridriksson” in the Norwegian Sea and surrounding waters, 1 July–10 August 2012. Working Document to Working Group of Widely Distributed Stocks, ICES, Lowestoft, UK, 21–27 August 2012. 45 pp.
- Nøttestad, L., Utne, K. R., Anthonypillai, V., Tangen, Ø., Valdemarsen, J. W., Oskarsson, G., Sveinbjørnsson, S., et al. 2013. Cruise Report from the Coordinated Ecosystem Survey (IESSNS) with M/V “Libas”, M/V “Eros”, M/V “Finnur Friði” and R/V “Arni Fridriksson” in the Norwegian Sea and surrounding waters, 2 July–9 August 2013. Working Document to Working Group of Widely Distributed Stocks, ICES, Copenhagen, Denmark, 27 August– 2 September 2013. 42 pp.
- Nøttestad, L., Salthaug, A., Johansen, G. O., Anthonypillai, V., Tangen, Ø., Utne, K. R., Sveinbjørnsson, S., et al. 2014. Cruise Report from the Coordinated Ecosystem Survey

(IESSNS) with M/V “Brennholm”, M/V “Vendla”, M/V “Finnur Friði” and R/V “Arni Fridriksson” in the Norwegian Sea and surrounding waters, 2 July–12 August 2014. Working Document to Working Group of Widely Distributed Stocks, ICES, Copenhagen, Denmark, 26 August – 1 September 2014. 49 pp.

- Nøttestad, L., V. Anthonypillai, G. Oskarsson, S. Þ. Jónsson, E. í. Homrum, et al., 2015. Cruise report from the International Ecosystem Summer Survey in the Nordic Seas (IESSNS) with M/V “Brennholm”, M/V “Eros”, M/V “Christian í Grótinum” and R/V “Árni Friðriksson”, 1 July - 10 August 2015. ICES Working Group on Widely Distributed Stocks (WGWISE), AZTI-Tecnalia, Pasaia, Spain, 25 – 31 August 2015. 48 p.
- Nøttestad, L., Anthonypillai, V., Tangen, Ø., Høines, Å., Utne, K. R., Oskarsson, G., Ólafsdóttir, A.H, et al. 2016c. Cruise Report from the International Ecosystem Summer Survey in Nordic Seas (IESSNS) with M/V “M. Ytterstad”, M/V “Vendla”, M/V “Tróndur í Gøtu”, M/V “Finnur Friði” and R/V “Arni Fridriksson” 1-31 July 2016. Working Document to Working Group of Widely Distributed Stocks, ICES, Copenhagen, Denmark, 31 August–6 September 2016. 41 pp.
- Nøttestad, L., Utne, K. R., Óskarsson, G. J., Jónsson, S. Þ., Jacobsen, J. A., Tangen, Ø., Anthonypillai, V., et al. 2016a. Quantifying changes in abundance, biomass and spatial distribution of Northeast Atlantic (NEA) mackerel (*Scomber scombrus*) in the Nordic Seas from 2007 to 2014. ICES Journal of Marine Science, 73: 359–373.
- Nøttestad, L., Diaz, J., Pena, H., Søiland, H., Huse, G., and Fernö, A. 2016b. The feeding strategy of mackerel in the Norwegian Sea in relation to currents, temperature and prey. ICES Journal of Marine Science 73(4), 1127-1137, doi:10.1093/icesjms/fsv239.
- Ólafsdóttir, A. H., Slotte, A., Jacobsen, J. A., Oskarsson, G. J., Utne, K. R., and Nøttestad, L. 2016. Changes in weight-at-length and size-at-age of mature Northeast Atlantic mackerel (*Scomber scombrus*) from 1984 to 2013: effects of mackerel stock size and herring (*Clupea harengus*) stock size. ICES Journal of Marine Science, 73: 1225–1235.
- Óskarsson, G.J., Gudmundsdóttir, A., Sveinbjörnsson, S., and Sigurdsson, Þ. 2016. Feeding ecology of mackerel and dietary overlap with herring in Icelandic waters. Marine Biology Research, 12: 16–29.
- Pacariz, S. V., Hátún, H., Jacobsen, J. A., Johnson, C., Eliassen, S., and Rey, F. 2016. Nutrient-driven poleward expansion of the Northeast Atlantic mackerel (*Scomber scombrus*) stock: A new hypothesis. Elementa Science of the Anthropocene, 4: 000105. DOI: 10.12952/journal.elementa.000105.
- Poloczanska, E. S., Brown, C. J., Sydeman, W. J., Kiessling, W., Schoeman, D. S., Moore, P. J., Brander, K., et al. 2013. Global imprint of climate change on marine life. Nature Climate Change, 3: 919–925.



- Prokopchuk, I., and Sentyabov, E. 2006. Diets of herring, mackerel, and blue whiting in the Norwegian Sea in relation to *Calanus finmarchicus* distribution and temperature conditions. ICES Journal of Marine Science, 63: 117–127.
- R Core Team. 2012. R: A language and environment for statistical computing. R Foundation for Statistical Computing, Vienna, Austria. ISBN 3-900051-07-0, URL <http://www.R-project.org/>.
- R Core Team. 2014. R: A language and environment for statistical computing. R Foundation for Statistical Computing, Vienna, Austria. Version 3.1.1. URL: <http://www.R-project.org/>.
- Rand, K.M, Beauchamp, D.A. and Lowe. S.A. 2010. Longitudinal Growth Differences and the Influence of Diet Quality on Atka Mackerel of the Aleutian Islands, Alaska: Using a Bioenergetics Model to Explore Underlying Mechanisms. Marine and Coastal Fisheries: Dynamics, Management, and Ecosystem Science, 2:1, 362–374, DOI: 10.1577/C09-046.1.
- Rey, F. 2012. Declining silicate concentrations in the Norwegian and Barents Seas. ICES Journal of Marine Science, 69: 208–212.
- Reynolds, R. W., and Smith, T. M. 1995. A high-resolution global sea surface temperature climatology. Journal of Climate, 8: 1571–1583.
- Reynolds, R. W., Rayner, N. A., Smith, T. M., Stokes, D. C., and Wang, W. 2002. An improved in situ and satellite SST analysis for climate. Journal of Climate, 15: 1609–1625.
- Schlesinger, M. E. and Ramankutty, N. 1994. An oscillation in the global climate system of period 65–70 years. Nature, 367: 723–726.
- Secor, D. H. 2015. Migration ecology of marine fishes. Johns Hopkins University Press, Baltimore. 292 pp.
- Shepherd, T. D., and Litvak, M. K. 2004. Density-dependent habitat selection and the ideal free distribution in marine fish spatial dynamics: considerations and cautions. Fish and Fisheries, 5: 141–152.
- Sundby, S. and Nakken, O. 2008. Spatial shifts in spawning habitats of Arcto-Norwegian cod related to multidecadal climate oscillations and climate change. ICES Journal of Marine Science, 65: 953–962.
- Trenkel, V. M., Huse, G., Mackenzie, B. R., Alvarez, P., Arrizabalaga, H., Castonguay, M., Goni N. *et al.* 2014. Comparative ecology of widely distributed pelagic fish species in the North Atlantic: implications for modelling climate and fisheries impacts. Progress in Oceanography, 129, 219–243.
- Uriarte, A. and Lucio, P. 2001. Migration of adult mackerel along the Atlantic European shelf edge from a tagging experiment in the south of the Bay of Biscay in 1994. Fisheries Research, 50: 129–139.

- Utne, K. R., Huse, G., Ottersen, G., Holst, J. C., Zabavnikov, V., Jacobsen, J. A., Óskarsson, G. J. *et al.* 2012. Horizontal distribution and overlap of planktivorous fish stocks in the Norwegian Sea during summers 1995-2006. *Marine Biology Research*, 8: 420–441.
- van der Kooij, J., Fässler, S. M.M., Stephens, D., Readdy, L., Scott, B. E., and Roel, B. A. 2016. Opportunistically recorded acoustic data support Northeast Atlantic mackerel expansion theory. *ICES Journal of Marine Science*, 73: 1115–1126.
- Wood, S.N. 2006. *Generalized Additive Models: An Introduction with R*. Chapman and Hall/CRC. 410 pp.
- Zar, J. H. 1999. *Biostatistical Analysis* 4<sup>th</sup> ed. Prentice-Hall, New Jersey. 663 pp.
- Zuur, A. F., Ieno, E. N., Walker, N. J., Saveliev, A. A., and Smith, G. M. 2009. *Mixed Effects Models and Extensions in Ecology with R*. Ed. By M. Gail, K. Krickeberg, J. M. Samet, A. Tsiatis, and W. Wong. Springer Science and Business Media, New York. 574 pp.

## Tables and Figures

### Figures:

**Fig. 1.** Mackerel traditional summer feeding area in the Norwegian Sea (light grey shade) from the late 1970s to 2006, and the core northward (dark grey shade) and the core westward (medium grey shade) expansion areas (Belikov et al., 1998; Uriarte and Lucio, 2001; Iversen, 2002; Utne et al., 2012; ICES, 2013, 2015; Nøttestad et al., 2016a). The core northward and the core westward areas were used for historical analysis of remotely sensed sea surface temperatures (SST). Area boundaries follow 1° grid lines, for longitude and latitude, as SST values were provided for such a grid. Also displayed are bathymetry contours, for 200 m, 1000 m and 2000 m depth, and the main surface currents in the Northeast Atlantic, the cold East Greenland current (blue) and the warm Atlantic current (red) (Blindheim and Østerhus, 2005).

**Fig. 2.** Mackerel density at surface trawl stations from IESSNS in 2007 and from 2010 to 2016 (a-h). Also displayed is centre-of-gravity (COG) calculated separately for the westward expansion area (west of 10°W; red triangle) and the Norwegian Sea (east of 10°W; red cross). The boundary between the Norwegian Sea and the westward expansion area is shown as a vertical red line. In the Norwegian Sea, COG calculations were limited to stations north of latitude 62°N (horizontal red line). COG was not calculated in the Norwegian Sea in 2011 due to limited survey coverage for latitudes north of 68°N. The boundaries between the traditional feeding grounds and the northward expansion area are also shown (broken black line).

**Fig. 3.** Mackerel weight-at-length for individuals caught in IESSNS in 2007 and from 2010 to 2016 ( $n = 103\ 750$ ) with regression line (grey solid line) which is  $\log_{10}\text{weight} = 2.905 \cdot \log_{10}\text{length} - 1.896$ ,  $R^2 = 0.90$ .

**Fig. 4.** The correlation between mackerel geographical distribution range (a), and centre-of-gravity (COG), calculated separately for the Norwegian Sea (b; north of 62°N and east of 10°W) and the westward expansion area (c; west of 10°W), and mackerel spawning stock biomass (SSB), from 1997 to 2016. Information not available for 1999-2001, 2004, 2005, 2008, 2009 and 2011.

**Fig. 5.** A box-whisker plot of mackerel density at stations with mackerel present in the traditional feeding area in the Norwegian Sea, in the northward and the westward expansion areas, from IESSNS in 2007 and from 2010 to 2016. For the box-whisker plot, first and third quartiles (the box), median (horizontal line within box), maximum and minimum (whiskers  $< 1.5 \cdot$  interquartile range) are showed but outliers are not. Survey coverage was limited in the northern Norwegian Sea in 2011 hence excluded.

**Fig. 6.** The quotient values (solid black circle) for mackerel frequency of occurrence (a) and for mackerel density (b), when present, in relation to temperature using data collected during IESSNS in 2007 and from 2010 to 2016. Also displayed is the quotient (horizontal black line) for an even distribution of mackerel across all categories with its 95% CI (dashed black line). For panel (b) display of upper CI is limited to values below 1.4. Number of stations per temperature

category, each category 1 °C (0.00 – 0.99°C, 1.00 – 1.99°C, *etc.*), is displayed by vertical bars.

**Fig. 7.** Temperature, at 10 m depth, at surface trawl stations both with mackerel present (solid circle) and absent (cross) from IESSNS in 2007, and from 2010 to 2016 (a-h). The traditional feeding grounds (shaded grey area), the westward expansion area (westward of the broken black line), and the northward expansion area (eastward of the broken black line and northward of the shaded grey area) are shown.

**Fig. 8.** Mesozooplankton abundance at surface trawl stations both with mackerel present (solid circle) and absent (cross) from IESSNS from 2010 to 2016 (a-g). The traditional feeding grounds (shaded grey area), the westward expansion area (westward of the broken black line), and the northward expansion area (eastward of the broken black line and northward of the shaded grey area) are shown.

**Fig. 9.** The quotient values (solid black circle) for mackerel frequency of occurrence (a) and for mackerel density (b), when present, in relation to mesozooplankton dry weight using data collected during IESSNS from 2010 to 2016. Also displayed is the quotient (horizontal black line) for an even distribution of mackerel across all categories with its 95% CI (dashed black line). Number of stations per mesozooplankton category, each category 2 g (0.00 – 1.99 g m<sup>-2</sup>, 2.00 – 3.99 g m<sup>-2</sup>, *etc.*), is displayed by vertical bars.

**Fig. 10.** Smoothed fits of explanatory variables from the best GAM of mackerel occurrence (a-b; n = 1534) and mackerel density (c; n = 1286), when present, using all trawl stations where both temperature and mesozooplankton density was measured from 2010 to 2016. Shaded grey band is the 95% confidence bound of the smoothing function and tick marks on the x-axis are the observed data points.

**Fig. 11.** GAM model predictions for mackerel density (best model from Table 2), for an area defined by latitude 56-75°N and longitude 47°W-30°E using a spatial grid resolution of 0.5 longitudes and 0.1 latitudes. The model was run using the average value of all stations for day-of-year (202), SSB was the average for 2010 to 2016 which was 4.6 million metric ton, temperature and mesozooplankton abundance was predicted by GAM.

**Fig. 12.** The average ( $\pm 95\%$  CI) monthly remotely sensed sea surface temperature in May (light grey square), June (dark grey triangle) and July (black circle), from 1997 to 2016 (NOAA/OAR/ESRL PSD, Boulder, CO, USA), for the core northward (a; n = 82 per year) and the core westward (b; n = 53 per year) expansion areas. Filled symbols are the years before mackerel range expansion began and open symbols are the years after the expansion began. Horizontal lines indicate the monthly means for all years. Background colours indicate the results from the univariate quotient analysis, namely the preferred temperature range for high mackerel density (dark grey), low mackerel density (light grey).

**Fig. 13.** A box-whisker plot of mackerel relative mean weight-at-length at surface trawl stations in the traditional feeding area in the Norwegian Sea, in the northward and the westward

expansion areas, from IESSNS in 2007, and from 2010 to 2016. For the box-whisker plot, first and third quartiles (the box), median (horizontal line with in box), maximum and minimum (whiskers  $< 1.5 \times$  interquartile range) are showed but outliers are not. IESSNS coverage was limited in the northern Norwegian Sea in 2011 hence excluded.

**Fig. 14.** Smoothed fits of explanatory variables from the best GAM of mackerel relative weight-at-length (a-c;  $n = 1286$ ) using all trawl stations where both temperature and mesozooplankton abundance were measured from 2010 to 2016. Shaded grey band is the 95% confidence bound of the smoothing function and tick marks on the x-axis are the observed data points.

**Fig. 15.** GAM model predictions for mackerel relative weight-at-length (best model from Table 3) for an area defined by latitude 56-75°N and longitude 47°W-30°E, using a spatial grid resolution of 0.5 longitude and 0.1 latitude. The model was run using the average spawning stock biomass from 2010 to 2016, which was 4.6 million ton. Temperature and mesozooplankton abundance predicted by GAM.

#### Supplementary Tables online:

**Table S1.** The 30 IESSNS conducted by Norway (NO), Iceland (IS), Greenland (GL) and Faroe Islands (FO) in 2007 and from 2010 to 2016. The surveys utilize both research vessels (R/V) and commercial pelagic vessels (M/V). Horizontal trawl opening is the average per survey or per year.

**Table S2.** Number of stations for surface trawling, temperature and mesozooplankton measurements during the IESSNS in Nordic Seas in 2007 and from 2010 to 2016. In brackets are number of stations with mackerel present.

#### Supplementary Figures online:

**Fig. S1.** GAM model residuals (positive are red and negative are black) for mackerel presence (a), density (b) and relative mean weight-at-length (c) using data from surface trawl stations where both temperature and mesozooplankton from 2010 to 2016 for the best models presented in Tables 2 and 3. Symbol size reflects residual value, *i.e.* greater value has larger symbol.

**Fig. S2.** A contour map of mackerel density at surface trawl stations with mackerel present (cross), from IESSNS in 2007 and from 2010 to 2016 (a-h). The traditional feeding grounds (area defined by a broke grey line), the westward expansion area (westward of the vertical broken grey line), and the northward expansion area (northward of the traditional feeding area and eastward of the vertical broken grey line) are shown.

**Fig. S3.** Mackerel mean relative weight-at-length at surface trawl stations (mean of all individuals caught per station) from IESSNS in 2007 and from 2010 to 2016 (a-h). The traditional feeding grounds (shaded grey area), the westward expansion area (westward of the

broken black line), and the northward expansion area (eastward of the broken black line and northward of the shaded grey area) are shown.

**Table 1.** The correlation between mackerel geographical distribution during summer in Nordic Seas, measured as area occupied and centre-of-gravity, and spawning stock biomass (SSB) from 1997 to 2016. Correlation for centre-of gravity are calculated separately for the northward shift (latitude °N) in the Norwegian Sea (east of 10°W) and for the westward (longitude °W) shift in the westward expansion area (west of 10°W). Total area is the sum of area occupied by mackerel both in the Norwegian Sea and in the westward expansion area.

	$\tau^*$	p-value	N
Geographical distribution	0.85	< 0.001	12 <sup>a</sup>
Center-of-gravity (latitude °N)	0.82	< 0.001	12 <sup>a</sup>
Center-of-gravity (longitude °W)	0.77	< 0.001	18 <sup>b</sup>

\*Kendall rank correlation coefficient with correction for ties and p-value from significance test of correlation (McLeod, 2011).

<sup>a</sup>Excluding years: 1999-2001, 2004, 2005, 2008, 2009, and 2011.

<sup>b</sup>Excluding years: 2008 and 2009.

**Table 2.** GAM fits comparison and model selection for the effects of ambient temperature ( $T$ ), mesozooplankton abundance ( $Z$ ), and spawning stock biomass (SSB) on mackerel presence (1) and on mackerel density (2) accounting for effects of location ( $lat$ ,  $lon$ ) utilizing IESSNS data for the period from 2010 to 2016. The best model, according to the parsimony principle, displayed in bold and its model parameters (3-4).

(1) Model presence <sup>*</sup>	$\Delta AIC$	Deviance explained (%)	UBRE score
<b><math>P \sim s(lat, lon) + s(T) + s(log_{10}(Z)) + SSB</math></b>	<b>0</b>	<b>47.0</b>	<b>-0.482</b>
$P \sim s(lat, lon) + s(T) + SSB$	15.5	45.6	-0.472
$P \sim s(lat, lon) + s(log_{10}(Z)) + SSB$	103.4	38.7	-0.414
$P \sim s(lat, lon) + s(T) + s(log_{10}(Z))$	9.25	46.1	-0.476
$P \sim s(lat, lon) + s(T)$	21.8	44.8	-0.468
$P \sim s(lat, lon) + s(log_{10}(Z))$	113.7	37.7	-0.408
$P \sim s(lat, lon) + SSB$	122.0	36.9	-0.402
(2) Model density <sup>**</sup>			GCV score
<b><math>Log_{10}(D) \sim s(lat, lon) + s(T) + s(log_{10}(Z)) + SSB</math></b>	<b>0</b>	<b>31.8</b>	<b>0.635</b>
$Log_{10}(D) \sim s(lat, lon) + s(T) + SSB$	4.2	31.0	0.637
$Log_{10}(D) \sim s(lat, lon) + s(log_{10}(Z)) + SSB$	81.7	26.9	0.676

$\text{Log}_{10}(D) \sim s(\text{lat}, \text{lon}) + s(T) + s(\text{log}_{10}(Z))$	9.8	31.2	0.640
$\text{Log}_{10}(D) \sim s(\text{lat}, \text{lon}) + s(T)$	15.6	30.3	0.642
$\text{Log}_{10}(D) \sim s(\text{lat}, \text{lon}) + s(\text{log}_{10}(Z))$	97.0	25.9	0.684
$\text{Log}_{10}(D) \sim s(\text{lat}, \text{lon}) + \text{SSB}$	85.2	26.2	0.678
(3) Parameters presence	estimated	standard error	p-value
<i>SSB</i>	0.9	0.29	0.001
(4) Parameters density			
intercept	4.6	0.67	< 0.001
<i>SSB</i>	0.5	0.15	0.001

$\Delta\text{AIC} = \text{AIC} - \text{minAIC}$

\*family is binomial; link function is logit; number of sampling stations = 1534

\*\*family is gaussian; link function is identity; number of sampling stations = 1286

**Table 3.** GAM fits comparison and model selection (1) for the effects of ambient temperature ( $T$ ), mesozooplankton abundance ( $Z$ ), and spawning stock biomass ( $\text{SSB}$ ) on mackerel relative mean weight-at-length ( $WL$ ) accounting for effects of location ( $\text{lat}$ ,  $\text{lon}$ ) and sampling day of year ( $\text{DOY}$ ) utilizing IESSNS data for the period from 2010 to 2016. Best model according to the parsimony principle displayed in bold and its parameters (2) are also displayed.

(1) Model	$\Delta\text{AIC}$	Deviance explained (%)	GCV score
$WL \sim s(\text{lat}, \text{lon}) + s(\text{DOY}) + s(\text{log}_{10}(D)) + s(T) + s(\text{log}_{10}(Z)) + \text{SSB}$	1.06	44.6	321.4
<b><math>WL \sim s(\text{lat}, \text{lon}) + s(\text{DOY}) + s(\text{log}_{10}(D)) + s(T) + \text{SSB}</math></b>	<b>0</b>	<b>44.5</b>	<b>321.1</b>
$WL \sim s(\text{lat}, \text{lon}) + s(\text{DOY}) + s(\text{log}_{10}(D)) + s(\text{log}_{10}(Z)) + \text{SSB}$	3.32	44.4	322.0
$WL \sim s(\text{lat}, \text{lon}) + s(\text{DOY}) + s(\text{log}_{10}(D)) + s(T) + s(\text{log}_{10}(Z))$	67.6	41.3	338.8
$WL \sim s(\text{lat}, \text{lon}) + s(\text{DOY}) + s(T) + s(\text{log}_{10}(Z)) + \text{SSB}$	86.9	40.0	344.1
$WL \sim s(\text{lat}, \text{lon}) + s(\text{DOY}) + s(\text{log}_{10}(D))$	98.2	39.6	347.3
$WL \sim s(\text{lat}, \text{lon}) + s(\text{DOY}) + s(T)$	163.5	36.0	365.6
$WL \sim s(\text{lat}, \text{lon}) + s(\text{DOY}) + s(\text{log}_{10}(Z))$	178.9	35.2	370.0
$WL \sim s(\text{lat}, \text{lon}) + s(\text{DOY}) + \text{SSB}$	94.2	39.5	346.0

(2) Parameters	estimated	standard error	p-value
<i>intercept</i>	-65.7	7.14	< 0.001
<i>SSB</i>	14.2	1.57	< 0.001

$\Delta AIC = AIC - \min AIC$

\*family is gaussian; link function is identity; number of sampling stations = 1256

